Designing heavy metal oxide glasses with threshold properties from network rigidity

Shibalik Chakraborty,[1] P. Boolchand,[1] M. Malki,[2,3] and M. Micoulaut[4]
[1]*School of Electronics and Computing Systems, College of Engineering and Applied Science, University of Cincinnati, Cincinnati, Ohio 45221-0030, USA*
[2]*CEMHTI, CNRS UPR 3079, 1D, Avenue de la Recherche Scientifique, 45071 Orleáns Cedex 02, France*
[3]*Université d'Orléans (Polytech' Orléans), BP 6749, 45072 Orléans Cedex 02, France*
[4]*Laboratoire de Physique Théorique de la Matière Condensée, Université Pierre et Marie Curie, 4 Place Jussieu, F-75252 Paris Cedex 05, France*

(Received 30 September 2013; accepted 9 December 2013; published online 3 January 2014)

Here, we show that a new class of glasses composed of heavy metal oxides involving transition metals (V_2O_5–TeO_2) can surprisingly be designed from very basic tools using topology and rigidity of their underlying molecular networks. When investigated as a function of composition, such glasses display abrupt changes in network packing and enthalpy of relaxation at T_g, underscoring presence of flexible to rigid elastic phase transitions. We find that these elastic phases are fully consistent with polaronic nature of electronic conductivity at high V_2O_5 content. Such observations have new implications for designing electronic glasses which differ from the traditional amorphous electrolytes having only mobile ions as charge carriers. © *2014 AIP Publishing LLC*. [http://dx.doi.org/10.1063/1.4855695]

I. INTRODUCTION

Only one element of the Periodic Table (Se) vitrifies at ambient pressure but a large number of glassy alloys can be obtained by combining appropriate elements from Group III, IV, and V with Group VI elements (O, S, Se, and Te) such as silica (SiO_2) or germanium diselenide ($GeSe_2$). In the design of physical, chemical, or electrical properties, these base network glasses are then alloyed with appropriate modifiers (e.g., Na_2O) or additives (AgI).[1] Molecular structure of the base network glasses is a prerequisite to develop a basic understanding of a structure-property relationship. The optimization of functionalities upon modification with alkali–oxides or electrolyte additives is then realized on an empirical basis, given the fact that the number of possible combinations is infinite. Another challenge is the absence of any precise information on the microscopic origin of the glass-forming ability itself, the resistance towards crystallization and the kinetics of glass transition. Therefore, only few attempts have really been made[2–5] to obtain glasses from important additives such as transition elements. As a result, the latter usually appear as minor additives for selected applications. For instance, Titania (TiO_2) with <1 mol. % is used for photo-active applications[6] such as self-cleaning coatings while Chromia (Cr_2O_3) has been used for centuries as a pigment for the green coloring of silicate glasses.[7]

Can network glasses be realized with large fraction of transition metal-oxides ? This knowledge appears to be essential for new applications that could emerge from detailed compositional studies, which would open an avenue to ultimately tune materials synthesis to specific applications. Here, we study thermal properties of heavy metal oxide glasses (HMO), composed of TeO_2 and V_2O_5. Telluria and vanadia as such are bad glass formers, but, their pseudo-binary alloys form excellent bulk glasses[8–10] over wide proportions ($18\% < x < 55\%$).

What is the origin of this remarkable behavior?

Currently this is not known. Here, we show for the first time that the glass forming ability in this family of HMO is topological in origin, and fundamentally derives from the onset of network rigidity. We arrive at the result by establishing a Maxwell stability criterion for isostatic rigid networks, since the nature of local structures of both TeO_2 and V_2O_5, and their evolution with composition are available from detailed nuclear magnetic resonance (NMR) experiments.[11]

Results show that TeO_2–V_2O_5 networks become optimally constrained near 20 mol. % of V_2O_5, and display experimentally all the features characteristic of two elastic phase transitions noted earlier in several network glasses; a stress-transition (stressed-rigid to rigid near $x = 23.5\%$) followed by a rigidity-transition (rigid to flexible near $x = 26.0\%$). The observation, to the best of our knowledge, is the first of its kind in a HMO. In addition, we find that electronic conductivity displays three regimes of variation with a threshold in electronic conduction near the rigidity transition ($x = 26.0\%$). Since electron transport is strongly tied to a local network deformation, one identifies its origin to be polaronic in character; it is promoted by a softening of the alloyed glass network once it enters the flexible phase with high vanadia content. It is believed that these results must be generic to the family of HMO containing the transition metal oxide V_2O_5. These new results open for the first time a promising extension of concepts of topology and rigidity from chalcogenides[12] and modified oxides[13] to the case of HMO. In this context, the approach of topology and rigidity to decoding the functionality of chalcogenides- and oxide-glasses has already proved to be remarkably successful.[12,14]

II. EXPERIMENTAL

A. Bulk glass synthesis

Dry and 99.99% TeO_2 and V_2O_5, and puratronic grade B_2O_3 powders in the appropriate weight ratio were mixed in a N_2 gas purged glove box using a mortar and pestle. The presence of a few (5) mol. % of B_2O_3 into the tellurovanadate binary glasses suppresses any tendency of segregation. Batches of 2 g in size were then transferred in a box furnace, and the T increased to 750 °C and kept there for 5 h. Melts were then quenched on steel plates resulting in micaceous black pieces. These were encapsulated in evacuated (10^{-7} Torr) quartz tubing and reacted at 750 °C for 24 h, and then water-quenched. Glass samples were cycled through T_g to relieve stress due to melt quenching. The second step of reacting the starting materials for 24 h was necessary to homogenize melts/glasses as revealed by Raman scattering and volumetric measurements.[15,16]

B. Experimental characterization

Calorimetric measurements made use of a model 2920 modulated differential scanning calorimetry (m-DSC) from TA Instruments Inc. to examine glass transitions. All mDSC experiments used a scan rate of 3 °C/min, a modulation time period of 100 s, and modulation amplitude of 1 °C. A glass transition endotherm was deconvoluted[17] to establish the reversing and non-reversing heat flow. Here, T_gs are established from the inflexion point of the reversing heat flow step associated with the T_g endotherm. Typically, scans on glasses were initiated at T_g-75 °C, and scanned up in temperature to T_g+50 °C, followed by a cooling cycle, which permitted us to make a frequency correction[17] to the non-reversing heat flow, $\Delta H_{nr}(x)$.

Volumetric analysis made use of a quartz fiber and a digital balance. Using Archimedes' principle, we measured the mass density (ρ) of the glasses of typically 150 mg size using 200 proof ethanol. A Si single crystal was used as a standard to calibrate density of alcohol. A Ge single crystal was used to confirm the 1/4% accuracy on all $\rho(x)$ measurements. Molar volumes were deduced by inverting the $\rho(x)$ measurements.

C. Electrical dc conductivity

The complex impedance $Z^*(\omega)=Z^{'x;}(\omega)+Z'(\omega)$ was measured[44] by a Solartron SI 1260 impedance analyzer over the frequency range of 1 Hz–1 MHz. Several temperatures have been considered over the whole concentration range. Conductivity $\sigma^*(\omega)$ was deduced from the complex impedance $Z^*(\omega)$. The real part of the dielectric permittivity $\varepsilon'(\omega)$ was computed using the electrical modulus $M^*(\omega) = 1/\varepsilon^*(\omega) = i\omega\varepsilon_0/\sigma^*(\omega)$ where ε_0 is the permittivity of free space.

III. RESULTS

A. Location of the mean-field rigidity transition

We first consider the network structure of $xV_2O_5-(1-x)TeO_2$. An investigation from NMR[11] has shown that the increase of V_2O_5 content leads to a systematic change in network connectedness (Fig. 1), which results from a change in the nature of building blocks. This has been independently established from an X-ray study[18] showing the decrease of the Te coordination from 4 to 3 with addition of vanadia.

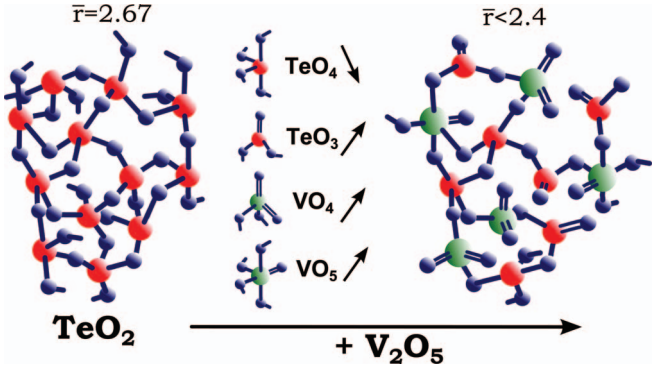

FIG. 1. Structural changes in heavy metal glasses. A schematic view of the structural changes induced by the vanadia into a base telluria glass network, following Ref. 11. The basic TeO_4 trigonal bipyramid (number of topological constraints $n_c = 3.67$, or mean coordination number, $\bar{r} = 2.67$) converts partially into $O = TeO_{2/2}$ trigonal pyramids TeO_3 ($n_c = 1.85$, $\bar{r} = 2.34$) while vanadia is present either in a tetrahedral VO_4 geometry ($n_c = 2.5$, $\bar{r} = 2.5$) or as an $O = VO_{4/2}(VO_5)$ trigonal bipyramid ($n_c = 3.5$, $\bar{r} = 3$). The average coordination number of the base network ($\bar{r} = 2.67$) is obviously reduced as the vanadia content increases. See Table I.

Static ^{125}Te NMR results have shown that there are three Te local structures populated in these glasses; two TeO_4 units and one TeO_3 unit. The TeO_4 units are composed of Te coordinated to 4 bridging oxygen in trigonal bipyramid (tbp) geometry, and the other a tbp unit having 3 bridging and 1 non-bridging oxygen (NBO) (Table I). These local structures are also detected from neutron X-ray scattering.[20] The TeO_3 unit is composed of Te having a NBO, a double bonded terminal O, and a bridging O. ^{51}V NMR results show occurrence of 4 V environments, two labeled as VO_5 and other two labeled as VO_4. Such structural changes have also been investigated and characterized from neutron scattering.[19,20] These have shown that typical distances appear in the first-neighbor peaks of the total correlation function that can be associated with different aforementioned geometries.

The VO_5 units consist, respectively, of V sites as in $(VO_4)_n^{3n-}$ chains and zig-zag $(V_2O_8)_{n-}$ zig-zag chains (Table I), while the two VO_4 units consist, respectively, of V sites as in VO_4^{3-} and in $(VO_3)_n^{n-}$ chains. From compositional

TABLE I. Summaries of Te- and V-local structures, corresponding count of constraints n_c and connectedness.

Specie	Constraint	Connectedness $\bar{r}$
$TeO_{4/2}$	3.67	2.67
$O_{1/2}Te(=O)–O^{\ominus}$	1.85	2.34
$O_{3/2}Te–O^{\ominus}$	3.0	2.34
$VO_4^{3\ominus}$	2.5	2.5
$(VO_3)_n^{n\ominus}$	2.5	2.5
$(VO_4)_n^{3\ominus}$	3.5	3
$(V_2O_8)_n$	3.87	3

studies, Sakida *et al.*[11] quantitatively established the populations of the three Te- and four V-centered local structures. These data permit the global connectivity and constraint count (n_c) of glasses to be established, as discussed below.

Specifically, the basic local structure of telluria composed of oxygen bridging $TeO_{4/2}$ trigonal bipyramids, is in fact progressively converted into an $O = TeO_{2/2}$ one, a quasi-trigonal Te with two bridging and one terminal (double bonded) oxygen, whereas the additive vanadia leads vanadium cation to exist in two environments: an $O = VO_{4/2}$ trigonal bipyramid with five oxygen-neighbors, and a VO_4 quasi-tetrahedra having two double bonded V=O bonds (Fig. 1). The concentrations of these building blocks depend on the V_2O_5 composition and converge at high vanadia content ($x > 30\%$) to the limit of 50% each.[11] These local structure results suggest that network connectivity systematically lowers due to the increased presence of terminal (double-bonded) oxygen; network mean coordination number ($\bar{r}$) decreases from $\bar{r} = 2.67$ at $x = 0$ to $\bar{r} = 2.45$ at $x = 80\%$ V_2O_5, a feature that is directly reflected in the compositional trend of the glass transition temperature $T_g(x)$ which usually reflects the change in network connectivity.[21] Calorimetric measurements show indeed $T_g(x)$ to monotonically decrease from 290 °C at $x = 18\%$ to 260 °C at $x = 35\%$ (Figure 2(a)). These findings provide the first clue that networks describing such glasses become steadily less connected as the vanadia content "x" increases, a tendency that has also been detected from the reduction of Te neighbors through diffraction measurements.[18–20] The starting TeO_2 system has a number of constraints equal to $n_c = 3.67$ indicating a stressed rigid nature of the network whereas at high vanadia content $VO_4^{3\ominus}$ and $(VO_3)_n^{n-}$ with both $n_c = 2.5$ (Table I) dominate.[11] With increasing vanadia content, one thus expects that a Maxwell stability criterion ($n_c = 3$) will occur at some point.

Using the species population determined by Sakida *et al.*,[11] we then proceed to enumerate the mean-field count of mechanical constraints $n_c(x)$ in these Telluro-Vanadate networks. For an atom possessing a coordination number r, the count of bond-stretching constraints (r/2), and of bond-bending constraints (2r − 3), for each atom possessing a coordination number of $r \geq 2$ allows obtaining the total $n_c(x)$. For terminal atoms, such as a double bonded terminal Oxygen in a TeO_3 unit, $r = 1$, only a bond-stretching constraint of 1/2 per atom is counted, according to rules established earlier.[22,23] The constraints of the 5% B_2O_3 are computed from a 3-fold boron and 2-fold bridging oxygen[24] but contribute weakly to the global count. We have thus obtained the global count of constraints $n_c(x)$ as a function of vanadia in the telluro-vanadate networks, and these results are plotted in Fig. 2(a), right axis. It is found that $n_c(x)$ starting from a value of about 3.44 near $x = 5\%$ steadily decreases to 2.73 near $x = 35\%$. These constraint estimates show that formation of the less connected, and therefore less constrained TeO_3 and VO_4 units at the expense of TeO_4 and VO_5 units lowers the global connectivity of these networks. Remarkably, the condition, $n_c = 3$, for rigidity percolation is realized when $x = 19.3\%$ (arrow in Fig. 2(a)), the Maxwell stability criterion for isostatic structures. These findings strongly suggest that the origin of glass formation in the present HMO is driven by

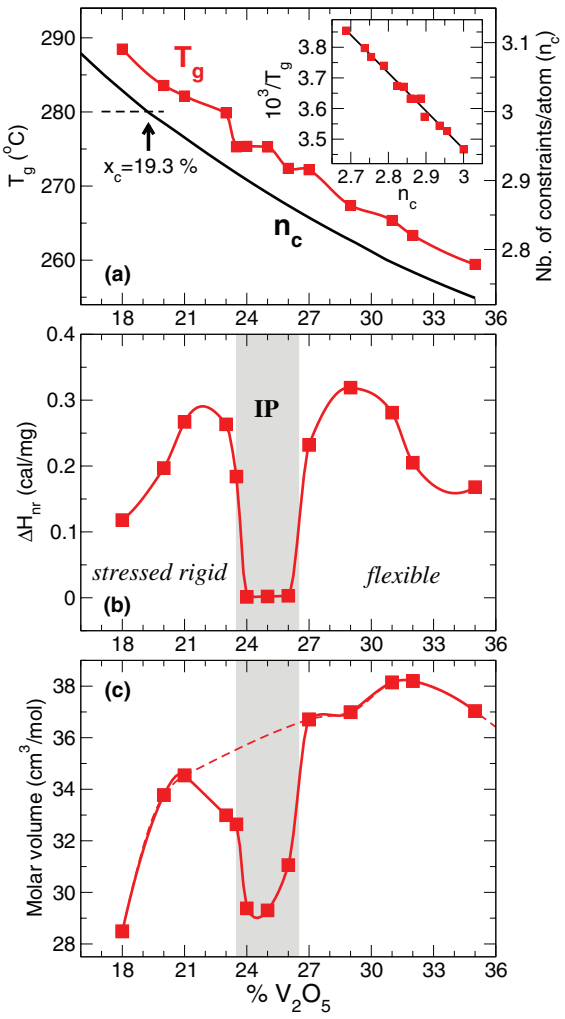

FIG. 2. Thermal properties of heavy metal glasses. Glass transition temperature (a), number of topological constraints ((a), right axis), non-reversing heat flow ΔH_{nr} (b), and molar volume variation (c) in $xV_2O_5-(95-x)TeO_2-5B_2O_3$ glasses as a function of vanadia content x. The square-well in thermal properties defines a reversibility window, similar to the ones in chalcogenide glasses. The glass transition variation (a) can be fitted (red curve) from the number of floppy modes f (right axis, $n_c = 3 - f$) in the network using a Lindemann criterion in combination with rigidity theory[25] (inset, see text for details). The arrow in (a) marks the Maxwell isostatic criterion determined from the species population of Sakida *et al.*[11]

the optimally coordinated nature of these networks. Using the mean-field approach of topological constraint count, we thus view networks at $x < 18\%$ to be in the stressed-rigid phase ($n_c > 3$), while those at $x > 19.3\%$ to be in the flexible ($n_c < 3$) phase, and the composition of $x = x_c = 19.3\%$ to be near the phase boundary between flexible and stressed-rigid glasses.

Furthermore, the reduction of the number of floppy mode density $\mathcal{F}(x) = 3 - n_c(x)$ is consistent with the obtained trend in glass transition temperature (Fig. 2(a)). Using a Lindemann criterium for the glass transition temperature, Naumis[25] has shown that T_g actually scales as

$$T_g = \frac{T_g(f=0)}{1+\alpha(3-n_c)}, \tag{1}$$

where α is a fitting parameter related to the vibrational properties of the stressed-rigid glass.[25] When the obtained computation of n_c using the statistics of species[11] and the B_2O_3

constraint count are put together with the measured values of T_g, it appears that Eq. (1) holds given that $1/T_g$ scales linearly with n_c (Fig. 2(a) inset). From the measured value of $T_g(f = 0) = 288\,^{\circ}C$ (Fig. 2(a)), we obtain the fitted value $\alpha = 2.2$, quite close to values ($\alpha = 1.01$) found for chalcogenides.[25]

B. Thermal and calorimetric measurements

Calorimetric measurements reveal that the non-reversing enthalpy of relaxation ($\Delta H_{nr}(x)$) at T_g varies in a highly non-monotonic fashion (Figure 2(b)) with glass composition x; the term sharply drops and becomes minuscule as $x > x_c(1) = 23.5\%$, and remains so until $x > x_c(2) = 26.5\%$, when it suddenly increases back up to a value observed below the first threshold ($x_c(1)$). The square-well like behavior of the non-reversing heat flow constitutes signature of the glass transition becoming thermally reversing in the $x_c(1) < x < x_c(2)$ composition range, similar to previous findings[26,27] reported in more common glasses, is fully consistent with the percolative nature of stress and rigidity transitions.[28] Based on these previous examples, it is clear that the present HMO glasses are stressed-rigid at high telluria content, but become flexible at high vanadia content, consistent with a reduction of network connectivity that is produced from species having a lower connectedness (Table I). Compositional trends in molar volumes of glasses (Figure 2(c)) also show a non-monotonic variation, and decrease by about 15% upon a few percent added V_2O_5. Molar volumes, in general, increase with increasing vanadia content x of glasses, but are found to reduce in a spectacular fashion as $x > 23\%$ and to remain low up till $x > 26\%$ when they increase sharply to acquire a value that appears to be a smooth extrapolation (broken line in Fig. 2(b)) from the low values of $x < 23\%$. The almost square-well like drop of about 19% in $V_m(x)$ in this compositional range, appears to nearly coincide with the reversibility window ($\Delta H_{nr} \simeq 0$) obtained from calorimetric measurements. From a bond-stretching and bond-bending relaxation model, a correlation has been established[29] between the minimum of the enthalpic relaxation at the glass transition and the isostatic nature of the network. This allows us in identifying the obtained window in HMO with the conventional intermediate phase (IP) reported in many other chalcogenide and oxide glass systems.[12–14,17,23] Furthermore, the stress-free (isostatic) nature is tightly linked with the space filling nature of networks[30] formed in these special isostatic ($n_c \simeq 3$) compositional windows. The obtained minimum in molar volume (Fig. 2(c)) is therefore also indicative that HMO undergoes a flexible to stressed rigid transition across the IP. However, it should be noted that the location of the latter is slightly shifted to higher compositions when compared to the mean-field estimate of 19.3% for the flexible to rigid transition, a situation that has been encountered in other glass-forming systems[31–33] as well, and which has been analyzed from the presence of typical isostatic species.

C. Electrical properties

Finally, we provide measurements of the dc conductivity (σ_{dc}) at different temperatures. Figure 3 shows the behavior of σ_{dc} for selected compositions. At low vanadia content (18%–27%), weak changes in electrical transport are obtained with temperature, but an important growth is observed at larger compositions (35%). When plotted at a fixed temperature, the same trend of σ_{dc} is obtained with vanadia composition, i.e., a mild increase at $x < 22\%$–23%, a plateau behavior in the reversibility window, and a power-law increase of $\sigma \simeq (x - x_c(2))^p$ once $x > x_c(2) = 27\%$. Clearly, a substantial increase of electrical conduction is linked to the flexible nature of the network as we observe an increase by an order of magnitude with the addition of just 5%–10% V_2O_5 in the flexible elastic phase ($x > 27\%$).

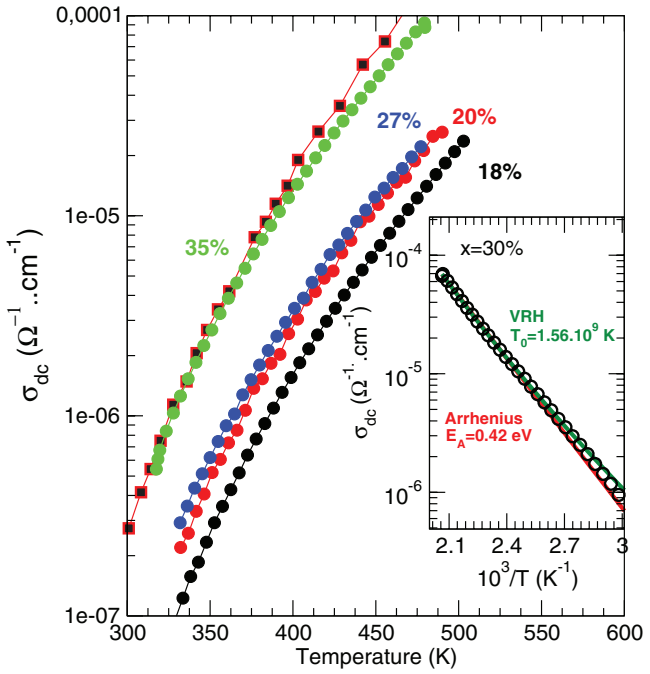

FIG. 3. DC conductivity in $xV_2O_5-(95-x)TeO_2-5\,B_2O_3$ glasses as a function of temperature for selected compositions (filled circles). The open squares (red) are results for a 20 V_2O_5–80 TeO_2 glass.[36] Inset: fits of the σ_{dc} conductivity data (circles) of $(1-x)TeO_2-xV_2O_5$ glasses ($x = 30\%$): Arrhenius fit $\sigma_{dc} = \sigma_0 \exp[-E_A/k_BT]$ (red curve) and variable-range-hopping conductivity[40] $\sigma_{dc} = \sigma_1 \exp[-(T_0/T)^{1/4}]$ (green curve). The fitted parameters T_0 and E_A are indicated.

Our results are actually of the same order as those obtained in a previous study on TeO_2–V_2O_5[35–37] (Figure 3), although a difference can be noticed that may arise from the incorporation of B_2O_3 in the present study.

The present data do not exhibit a signature of the stress transition found at 23.5% (Fig. 2) although we notice a moderate jump in conductivity σ between the 18% and 21% composition that may be assigned to the vanishing of stress as the network connectivity is decreased. It may be possible that the present temperature range (300–500 K, Fig. 3) is too high to make a stress transition detectable. Such a conclusion is supported from previous work on a solid electrolyte[26] showing that the jump in σ found at the stress transition decreases with increasing temperature (specifically Fig. 3a in Ref. 34). At high T, understandably, there is smoothing of the phase boundaries because the activation energy for diffusion decreases.

IV. POLARONS AND FLEXIBLE NETWORKS

As there are obviously no ions involved, sources contributing to the dc conduction mechanism can either arise from electrons or from polarons.[38] However, the measurement of the low temperature (300 K) relaxation of the dielectric constant ($\varepsilon' \simeq 40$–60 determined from the electrical modulus for all compositions) appears to be activated with a frequency of 0.1 MHz, a frequency which is by far too low to be associated with an electronic tunneling mechanism.[39] The only possible mechanism for charge transport is therefore polaronic in nature, which is, indeed, consistent with the presently established flexible nature of the network at high vanadia content. The activation energy for polaronic conduction usually arises from electron-lattice interactions and from static disorder.[37] Local network polarization and deformation or distortion caused by a moving electron is facilitated by the presence of floppy modes[25] in the elastically flexible (at x > 27%) phase. The observation is also consistent with the fact that Mott's variable-range-hopping (VRH) equation for polaronic conductivity[40,41] of the form $\sigma_{dc} = \sigma_0 \exp[-(T_0/T)^{1/4}]$ fits better the low temperature σ_{dc} experimental data than a standard Arrhenius equation $\sigma_{dc} = \sigma_0 \exp[-E_A/k_B T]$ (inset of Fig. 3), thus strongly confirming the polaronic nature of conduction as also emphasized in a previous study.[37] However, here it is found that it is mostly the network connectivity decrease which drives the onset of polaronic conduction due to the presence of a low connected flexible structure at high vanadia content.

The fit of $\sigma_{dc} = \sigma^*(0)$ with temperature has been performed over a range of temperatures. The variation of conductivity on an Arrhenius plot does not show a linear behavior exactly, deviations occur at high temperatures, typically at $10^3/T \simeq 2.55$, e.g., the 30% composition (Figure 3) corresponding to 392 K $\simeq 0.7\ T_g$. In contrast, a VRH model fit provides a better agreement over an extended temperature range, especially at low temperature where it applies.[40]

Furthermore, T_0 in the Mott VRH formalism is related to the hopping energy W and hopping range R of polarons via:

$$T_0 = \frac{24}{\pi k_B N(E_F) D^3}, \tag{2}$$

$$W = \frac{3}{4\pi R^3 N(E_F)}, \tag{3}$$

$$R^2 = \sqrt{\frac{D}{8\pi N(E_F) k_B T}}, \tag{4}$$

where D is the decay length of the localized wave-functions, usually the distance between two neighboring atoms, and $N(E_F)$ is the density of localized states at the Fermi level. The distance D is taken here equal to 2.76 Å which is the distance between two neighboring oxygen atoms, the typical distance involved in vanadates.[19,20,45] Both quantities W and R appear to capture well (inset of Fig. 4) the softening of the glass network by displaying a steep decrease of W(x) and a steep increase of R(x) in the reversibility window. It should also be stressed that the range of variation of the lattice-electron interaction W(x) (Fig. 4 inset) is of about 1.8–2.0 meV, i.e., of the order of the floppy mode energy (4 meV) that represents the cost in low energy deformations of flexible networks.[25,46] Local network deformations are accentuated in the flexible phase, and propagate easily in the glasses at x > 27%. We can thus understand that polaronic conduction is enhanced due to an increased number of floppy modes,[42,43] and activation barriers that are close to the floppy mode energy.

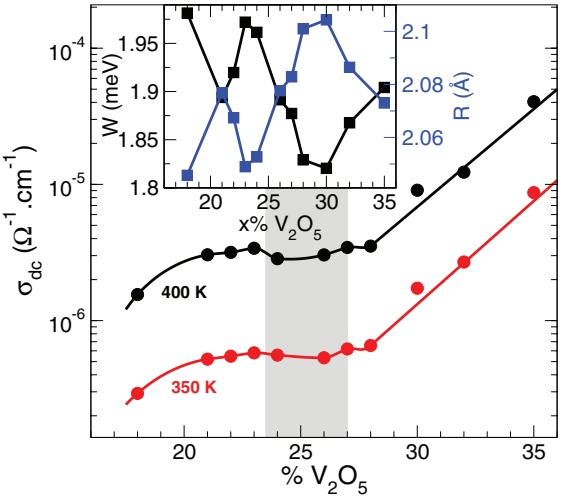

FIG. 4. Conductivity of present heavy metal oxide glasses. DC conductivity measurements (at 350 K and 400 K) in $xV_2O_5-(95-x)TeO_2$–5 $B2O_3$ glasses as a function of vanadia (V_2O_5) content x. The inset shows activation energies W(x) for polaron hopping energy, and corresponding hopping range R(x) using Mott's variable range hopping (VRH) equation (blue symbols, right axis).

V. CONCLUSION

Global consequences of the present findings can now be enunciated. In a fashion similar to those used in the usual modified-oxide and chalcogenide network glasses, it is the first time that concepts from topology and network connectivity have been used here to understanding the glass-forming tendency in HMO. This family of glasses has received much less attention up to now in this respect. A flexible to rigid transition is found in these telluro-vanadates which bears striking similarities with those found in other common glasses including commercial ones. Finally, using the established population of the cation species,[11] a mean-field constraint count has permitted identifying a rigid to flexible transition from the Maxwell stability criterion[42,43] at the composition of 19.3% vanadia. The location is found to be somewhat lower than the observed reversibility and molar volume window (23.5% < x < 27%) suggesting missing details in the way the structure organizes. However, we note that other glassy systems display the same tendency with deviations from the mean-field result.[31–33]

Finally, for the first time we show that an electronic transition takes place, which manifests in a power-law increase of the dc conductivity as the vanadia content exceeds the threshold value (27%). This transition is deeply connected to the rigid to flexible transition induced by the loss of connectivity as local structures with lower connectedness appear in

the networks. Electrical conductivity is polaronic in character, and increases precipitously due to floppy modes that facilitate electron transport through local deformations in the elastically flexible phase.

ACKNOWLEDGMENTS

We acknowledge support from NSF Grant No. DMR-08-53957. M.M. acknowledges support from the Franco-American Fulbright Commission, and International Materials Institute for financial support. P.B. acknowledges Professor Y. Dimitriev for introducing him to heavy metal oxide glasses.

[1]D. R. Uhlmann and N. J. Kreidl, *Glass Science and Technology* (Academic Press, New York, 1990).
[2]M. A. Sidkey, R. El Mallawany, R. I. Nakhla, and A. Abd El-Moneim, Phys. Status Solidi A **159**, 397 (1997).
[3]M. P. Kumar, T. Sankarappa, and A. M. Awasthi, Physica B **403**, 4088 (2008).
[4]S. Gupta and A. Mansingh, Philos. Mag. B **78**, 265 (1998).
[5]N. V. Ovcharenko, S. A. Cheboratev, V. V. Volkova, and A. K. Yakhkind, Fiz. Khim. Stekla **11**, 607 (1985).
[6]Y. Paz, Z. Luo, L. Rabenberg, and A. Heller, J. Mater. Res. **10**, 2842 (1995).
[7]R. K. Brow, J. Am. Ceram. Soc. **70**, C-129 (1987).
[8]M. A. Sidkey, R. El Mallawany, R. I. Nakhla, and A. Abd El-Moneim, J. Non-Cryst. Solids **215**, 75 (1997).
[9]E. P. Denton, H. Rawson, and J. E. Stanworth, Nature (London) **173**, 1030 (1954).
[10]R. A. El-Mallawany, *Tellurite Glasses* (CRC Press, 2001).
[11]S. Sakida, S. Hayakawa, and T. Yoko, J. Phys.: Condens. Matter **12**, 2579 (2000).
[12]P. Boolchand, P. Chen, and U. Vempati, J. Non-Cryst. Solids **355**, 1773 (2009).
[13]M. Micoulaut, Am. Mineral. **93**, 1732 (2008).
[14]K. Rompicharla, D. I. Novita, P. Chen, P. Boolchand, M. Micoulaut, and W. Huff, J. Phys.: Condens. Matter **20**, 202101 (2008).
[15]K. Gunasekera, S. Bhosle, P. Boolchand, and M. Micoulaut, J. Phys. Chem. **117**, 10027 (2013).
[16]S. Ravindren, K. Gunasekera, Z. Tucker, A. Diebold, P. Boolchand, and M. Micoulaut, e-print arXiv:1311.6385.
[17]P. Chen, P. Boolchand, and D. Georgiev, J. Phys.: Condens. Matter **22**, 065104 (2010).
[18]Y. Dimitriev and V. Dimitrov, Mater. Res. Bull. **13**, 1071 (1978).
[19]P. A. V. Johnson, A. C. Wright, C. A. Yarker, and R. N. Sinclair, J. Non-Cryst. Solids **81**, 163 (1986).
[20]U. Hoppe, E. Yousel, C. Rüssel, J. Neuefeind, and A. C. Hannon, Solid State Commun. **123**, 273 (2002).
[21]M. Micoulaut and G. G. Naumis, Europhys. Lett. **47**, 568 (1999).
[22]P. Boolchand and M. F. Thorpe, Phys. Rev. B **50**, 10366 (1994).
[23]Y. Wang, J. Wells, D. G. Georgiev, P. Boolchand, K. A. Jackson, and M. Micoulaut, Phys. Rev. Lett. **87**, 185503 (2001).
[24]J. C. Mauro, P. K. Gupta, and R. J. Loucks, J. Chem. Phys. **130**, 234503 (2009).
[25]G. G. Naumis, Phys. Rev. B **73**, 172202 (2006).
[26]D. I. Novita, P. Boolchand, M. Malki, and M. Micoulaut, Phys. Rev. Lett. **98**, 195501 (2007).
[27]M. Zhang and P. Boolchand, Science **266**, 1355 (1994).
[28]M. F. Thorpe, D. J. Jacobs, M. V. Chubynsky, and J. C. Phillips, J. Non-Cryst. Solids **266–269**, 859 (2000).
[29]M. Micoulaut, J. Phys.: Condens. Matter. **22**, 285101 (2010).
[30]C. Bourgel, M. Micoulaut, M. Malki, and P. Simon, Phys. Rev. B **79**, 024201 (2009).
[31]D. G. Georgiev, M. Mitkova, P. Boolchand, G. Brunklaus, H. Eckert, and M. Micoulaut, Phys. Rev. B **64**, 134204 (2001).
[32]P. Chen, C. Holbrook, P. Boolchand, D. G. Georgiev, and M. Micoulaut, Phys. Rev. B **78**, 224208 (2008).
[33]D. G. Georgiev, P. Boolchand, H. Eckert, M. Micoulaut, and K. Jackson, Europhys. Lett. **62**, 49 (2003).
[34]M. Micoulaut, M. Malki, D. I. Novita, and P. Boolchand, Phys. Rev. B **80**, 184205 (2009).
[35]B. W. Flynn, A. E. Owen, and J. M. Robertson, in *Proceedings of the 7th International Conference on Amorphous and Liquid Semiconductors*, edited by W. E. Spear (CICL, Edinburgh, 1977), p. 678.
[36]M. Levy, F. Rousseau, and M. J. Duclot, Solid State Ionics **28–30**, 736 (1988).
[37]V. K. Dhawan, A. Mansingh, and M. Sayer, J. Non-Cryst. Solids **51**, 87 (1982).
[38]S. Elliott, Adv. Phys. **36**, 135 (1987).
[39]C. Homes, T. Vogt, S. Shapiro, S. Wakimoto, and A. Ramirez, Science **293**, 673 (2001).
[40]N. Mott and E. Davis, *Electronic Processes in Non-Crystalline Materials* (Clarendon, Oxford, 1979).
[41]L. Zhang and Z.-J. Tang, Phys. Rev. B **70**, 174306 (2004).
[42]J. C. Phillips, J. Non-Cryst. Solids **34**, 153 (1979).
[43]J. Phillips, J. Non-Cryst. Solids **43**, 37 (1981).
[44]C. Simonnet, J. Phalippou, M. Malki, and A. Grandjean, Rev. Sci. Instrum. **74**, 2805 (2003).
[45]R. N. Sinclair, A. C. Wright, B. Bachra, Y. B. Dimitriev, V. V. Dimitrov, and M. G. Arnaudov, J. Non-Cryst. Solids **232–234**, 38 (1998).
[46]W. A. Kamitakahara, R. L. Cappelletti, P. Boolchand, B. Halfpap, F. Gompf, D. A. Neumann, and H. Mutka, Phys. Rev. B **44**, 94 (1991).